Design of Meloxicam and Lornoxicam Transdermal Patches: Preparation, Physical Characterization, *ex Vivo* and *in Vivo* Studies

Gülgün Yener,*[,a] Melike Üner,[a] Ümit Gönüllü,[a] Sinem Yildirim,[a] Pınar Kiliç,[a] Serap Sağlik Aslan,[b] and Aslı Barla[c]

[a] *Department of Pharmaceutical Technology, Faculty of Pharmacy, Istanbul University;* [b] *Department of Analytical Chemistry, Faculty of Pharmacy, Istanbul University; Beyazit, Istanbul 34116, Turkey: and* [c] *Aromsa Besin Aroma ve Katkı Maddeleri Sanayi ve Ticaret Anonim Şirketi; Gebze, Kocaeli 41480, Turkey.*

Received May 25, 2010; accepted August 6, 2010

Transdermal patches of meloxicam (MX) and lornoxicam (LX) were aimed to be prepared in order to overcome their side effects by oral application. The strategy was formulation of optimized films to prepare transdermal patches by determination of physical properties and investigation of drug–excipient compatibility. As the next step, *in vitro* drug release, assesment of anti-inflammatory effect on Wistar Albino rats, *ex vivo* skin penetration and investigation of factors on drug release from transdermal patches were studied. Hydroxypropyl methylcellulose (HPMC) was concluded to be suitable polymer for formulation of MX and LX transdermal films indicating pharmaceutical quality required. MX and LX transdermal patches gave satisfactory results regarding to the edema inhibition in the assessment of anti-inflammatory effect. MX was found out to be more effective compared to LX on relieving of edema and swelling. These results were supported by data obtained from *ex vivo* penetration experiments of drug through rat skin. Indicative parameters like log *P*, molecular weight and solubility constraint on penetration rate of drugs also indicated good skin penetration. Transdermal patches of MX and LX can be suggested to be used especially for the immediate treatment of inflammated area since it displays anti-inflammatory effect, soon.

Key words meloxicam; lornoxicam; transdermal delivery; transdermal patch; anti-inflammatory activity

Non-steroidal anti-inflammatory drugs (NSAIDs) are among the oldest drugs. Despite NSAIDs have been very often prescribed and they are generally over-the-counter medications, new structures and formulations have been introduced by various research groups and pharmaceutical industry. Cyclooxygenase-2 (COX-2) selective inhibitors as a new generation NSAIDs were introduced in the late 1990s since traditional NSAIDs have various potential risks including death. COX-2 inhibitors have been studied by examining their efficacy and advers reactions. They were found to cause lower gastrointestinal (GI) side effects compared to those of the others. However, clinical studies have also displayed that COX-2 inhibitors still had various risk factors depending on the dose. Meloxicam (MX) and lornoxicam (LX) are two of COX-2 inhibitors of the enolic acid class. They display their effects by inhibition of COX-1 isosyme mainly at higher doses.[1—4] Main side effects of MX and LX have been reported as abdominal pain, anemia, hepatitis, GI problems such as anorexia, dispepsia, ulceration, bleeding, perforation and constipation, dermatological problems such as dermatitis and photosensitivity.[5—7]

To overcome side effects caused by COX-2 inhibitors including MX and LX, transdermal applications introduce an alternative route. Inflammated area can be treated with a transdermal patch which also display sistemic effects. Transdermal patches allow drug penetration through skin in application site such as chest, inner forearm and ear back by addition of penetration enhancers to the formulations. These systems have a good patient compliance due to their easy application and finishing application whenever being needed. Drugs can be protected from the first pass metabolism as a very important advantage.[8,9]

In this study, transdermal patches of MX and LX were aimed to be prepared in order to overcome their side effects by oral application. MX and LX films were formulated. They were tested in order to ascertain their physical properties indicating pharmaceutical quality. For this aim, weight variation and thickness, mechanical strength, compatibility between drug and transdemal film excipients, variation in drug content and *in vivo* dissolution of the films were determined before preparation of their transdermal patches.[10] Then, anti-inflammatory effects of MX and LX incorporated into transdermal patches were evaluated by *in vivo* study on rats. Their effects were also compared to those of oral application on rats in order to find out anti-inflammatory potency of drugs by transdermal route. Data obtained from this study were discussed with *in vitro* drug release through artificial membrane and *ex vivo* study on drug penetration through rat skin.

Experimental

Materials MX and LX were obtained from Bilim İlaç Sanayi A.Ş. and Abdi İbrahim İlaç Sanayi ve Tic. A.S. (Turkey), respectively. Nitrocellulose membranes (0.45 μm) were purchased from Millipore (Turkey). 3M 9773 Foam Tape, CoTran 9719 Backing and Scotchpak 1020 Release Liner for preparing transdermal patch of films were kind gifts from 3M Drug Delivery Systems (Germany). Bio-Psa AC7-4201 which was used as a skin contact silicone adhesive for patches was kindly provided from Dow Corning Corp. (Turkey). Hydroxypropyl methylcellulose (HPMC) (Methocel K15 Premium EP) was obtained from Colorcon (Turkey). Carboxymethyl cellulose sodium (CMC-Na), propylene glycol (PG) and carrageenan (λ-carrageenan) were purchased from Sigma-Aldrich (Turkey). All other chemicals used were of analytical grade.

Preparation of Films and Transdermal Patches CMC-Na and HPMC were used for preparation of MX and LX films (Table 1). For this aim, aqueous polymer gel was prepared and kept at room temperature over night. Then, propylene glycol (PG) as a plasticizer agent was added under stirring using a HS-100D propeller mixer (Daihan Scientific, Korea) at 500 rpm. Certain amount of drug was suspended in water (1 : 5) and it was added to the gel mixture under stirring using the propeller mixer at 500 rpm. After the mixture was kept in an ultrasonic bath (Bersonic, Turkey) for elimination of air bubbles, it was homogenously poured into a petri dish (100×20 mm) and dried in a WiseVen Fuzzy Control System at 40±2 °C (Daihan Scientific,

* To whom correspondence should be addressed. e-mail: gulyen@superonline.com

Table 1. Constituents (%) of MX and LX Films

Formulations	Constituents (%)				
	MX	LX	CMC-Na	HPMC	PG
MX-CMC-7.5	1	—	3	—	7.5
MX-CMC-10	1	—	3	—	10
MX-HPMC-7.5	1	—	—	3	7.5
MX-HPMC-10	1	—	—	3	10
LX-CMC-7.5	—	1	3	—	7.5
LX-CMC-10	—	1	3	—	10
LX-HPMC-7.5	—	1	—	3	7.5
LX-HPMC-10	—	1	—	3	10

Korea). Films obtained were physically characterized and a few formulations were decided to be suitable for carrying out the study. Transdermal patches were then prepared by using those MX and LX films.

Films selected were cut in size of 3.15 cm^2 surface area. Transdermal patches were provided by using 3M 9773 Foam Tape, CoTran 9719 Backing, the film, a silicone skin contact adhesive (0.01 ml) (Bio-Psa AC7-4201) and Scotchpak 1020 Release Liner as transdermal patch components, respectively (Fig. 1).

Determination of Weight Variation, Thickness and Tensile Strength of Films Six pieces (1 cm×1 cm) were precisely cut from films. Pieces were weighed and their thickness were determined by using a micrometer (Mitutoyo, Japan).

Circle pieces with 4 cm diameter from films were cut and their tensile strengths were determined by using a TA-TX Plus Texture Analysis Apparatus (U.K.) equipped with a 0.25″ spherical probe (P/0.25 s). Rotation rates of the probe were 0.1 mm/s, 0.05 mm/s and 5.0 mm/s at pre-measurement, measurement and post-measurement stages, respectively. The measurement was performed under 200 g force with 5 kg loading chamber for 2 s. Strength of films was determined from force-time profiles obtained.

Fourier Transform Infrared Spectroscopy (FT-IR) Analysis FT-IR was carried out to assess the interaction between drugs and transdermal film excipients. For this aim, sufficient amounts of pure drugs (MX and LX) and their transdermal films in pieces with 0.5 cm diameter were scanned over a wave number range of 4000 to 650 cm^{-1} at resolution of 4 cm^{-1} in a Perkin Elmer 100 FT-IR instrument (U.K.) equipped with Perkin Elmer Spectrum Version 6.0.2 Software. The system was operated in the transmission mode. Sample was placed on the sample stage and 100 N force was applied for scanning.

Differential Scanning Calorimetry (DSC) Analysis Drug-excipient compatibility was investigated by DSC. DSC analysis was carried out on pure drugs and films in order to search possible interaction between drugs and film ingredients. 15—20 mg samples were weighed into standard sealed aluminium pans of the apparatus (Mettler TA 3000 Controller and DSC821^e, Mettler, Switzerland) and heated from 25 to 300 °C with a heating rate of 5 K/min flushing with 80 ml N_2/min. Holes were made in lids in order to allow dehydration of samples. Melting peaks and enthalpies were calculated using the Mettler Star software. Crystallization behaviours of drugs in transdermal films were investigated.

Determination of Drug Content of Films Circle pieces with 1 cm diameter cut from films were dissolved in 10 ml pH 7.4 phosphate buffer solution (PBS) in the ultrasonic bath for 30 min. Solutions were diluted to 25 ml and they were filtered through S&S^{5893} blue ribbon filter papers. Amounts of MX and LX in films were assayed spectrophotometrically at 272 nm and 376 nm (Shimadzu UV-1601 spectrophotometer, Japan), respectively.

***In Vitro* Dissolution Study from Films** *In vitro* dissolution test for transdermal patches reported in European Pharmacopoeiae 2008 was performed on pieces with 4 cm diameter cut from films. Pieces were fixed between the same sized glass disks and sieves with 125 μm opening. Nine hundred milliliters pH 7.4 PBS at 32±0.5 °C and 50 rpm rotation speed were used for this study. One milliliter samples were taken at predetermined time intervals and diluted to 10 ml. Solutions were assayed spectrophotometrically to determine MX and LX content after being filtered through S&S^{5893} blue ribbon filter paper.

***In Vitro* Drug Release Study from Transdermal Patches** Nitrocellulose membranes (0.45 μm) were used between two halves of Franz-type diffusion cells with 3.15 cm^2 surface area and 33.2 ml receptor volume containing pH 7.4 PBS. After fixing transdermal patches on membranes kept in pH 7.4 PBS over night, 1 ml samples were taken at predetermined time intervals. Drug release was determined spectrophotometrically after proper dilution of samples to 10 ml. Temperature of receptor phase was kept at 37±0.5 °C during the study. The amount of drug diffused at predetermined time intervals was calculated. Permeation coefficient (P) from membrane was calculated by using the following equation:

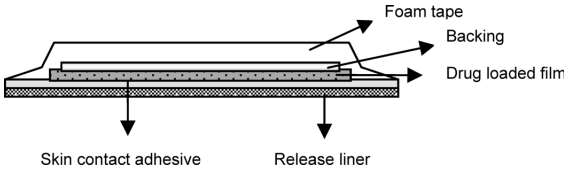

Fig. 1. Section of Transdermal Patches Prepared and Its Components

$$P = K \cdot H / A \quad (1)$$

where K is diffusion rate obtained from the slope of the linear drug diffusion profiles, H is the thickness of the film in cm and A is the surface area of the film in cm^2.[11] Release profiles were kinetically evaluated by using different models (zero order, first order and Higuchi square-root model) and the following equation derived by Korsmeyer *et al.*[12]:

$$M_t / M_\infty = K \cdot t^n \quad (2)$$

Where M_t/M_∞ is the fractional release of drugs, M_t is the released amount at release time t, M_∞ is the total amount of drugs contained in films, K is the kinetic constant and n is the diffusional release exponent indicative of the release mechanism.

***In Vivo* Study, Assessment of Anti-inflammatory Effects** Carrageenan induced rat hindpaw edema method were used on Wistar Albino rats (150—200 g) provided from DETAE, Istanbul University Institute for Experimental Medicine in this study. The animals were housed in plastic cages at a constant temperature (22±1 °C) and humidity (60±1%) under 12 h light–dark cycle. They were given standart laboratory diet and tap water *ad libitum*. Rats were acclimized to the laboratory at least 7 d prior to the experiments. The *in vivo* experimental protocol was approved by the Local Ethical Committee of Animal Experiments in Experimental Medical Research Institute of Istanbul University (07.11.2007, No: 18).

Animals were divided into 5 groups of 6 animals (Table 2). Left hindpaws of rats were measured with a blethysmometer and paw volumes (ml) were obtained. Group 1 was the blank which treated with 0.25% CMC-Na aqueos solution by oral route. MX and LX were suspended in water (0.1%) for oral application to Groups 2 and 4. Abdomens of Groups 3 and 5 were precisely shaved 2 d prior to the transdermal application. The inflammation was induced by intraplantar injection of 0.1 ml of a 1% carrageenan solution in saline (1%, w/v) in the left hindpaw of all rats 30 and 60 min later oral and transdermal applications (Groups 1—5), respectively. The intensity of edema was assessed by measuring the paw volume with the blethysmometer. Measurements were carried out at predetermined time intervals for 5 h. Swelling % and edema inhibition % were calculated by using Eqs. 3 and 4;

$$\text{swelling (\%)} = [(V_t - V_0)/V_0] \times 100 \quad (3)$$

$$\text{edema inhibition (\%)} = \{[(V_t - V_0)_{\text{control}} - (V_t - V_0)_{\text{application}}] / (V_t - V_0)_{\text{control}}\} \times 100 \quad (4)$$

V_0: mean volume of hindpaws before the application;
V_t: mean volume after drug application by oral and transdermal routes at time (t).

***Ex Vivo* Skin Penetration Study** Franz-type diffusion cells with 3.15 cm^2 surface area and 33.2 ml receptor volume containing pH 7.4 PBS were used for the skin penetration study. For this aim, shaved abdominal skins of Wistar Albino rats (150—200 g) were taken and underlying fatty tissue was removed by blunt dissection. Transdermal patches including 3.15 cm^2 films were applied on the surface of rat skins and were placed between two halves of cells. Penetration of drugs were assayed from samples collected at predetermined time intervals by HPLC.

The solubility constrain in the stratum corneum was calculated by the following equation:

$$\log \sigma_{sc} = 1.911(10^3/\text{mp}) - 2.956 \quad (5)$$

Table 2. Applications to Animals in the Assessment of Anti-inflammatory Effects

Groups	Application
1 (blank)	0.25% CMC-Na aqueous solution by oral route
2	MX aqueous suspension by oral route (12 mg/kg)
3	MX transdermal patch[a] on the abdominal region
4	LX aqueous suspension by oral route (12 mg/kg)
5	LX transdermal patch[b] on the abdominal region

Patches of *a*) MX-HPMC-10 and *b*) LX-HPMC-7.5 films.

where mp is the melting points of MX and LX as Kelvin.[13]

HPLC Analysis HPLC analysis was employed for determination of skin penetration of MX and LX from transdermal patches in *ex vivo* study on rat skins. For this aim, a Thermo Separation HPLC apparatus (U.S.A.) equipped with UV 3000 model dedector, AS 3000 autosampler, SN 4000 software and C18 Phenomenex (250×3.90 mm) column was used for determination of MX and LX amounts penetrated through skin. Mobile phase was KH_2PO_4 solution : acetonitril (55 : 45) (pH 2.5) was used at 1 ml/min flow rate. Injection volume was 20 μl. Calibration curve was gained from 6 solutions at 0.1—0.5 μg/ml concentration range by detection at 366 nm.

Data Treatment and Statistics Statistical evaluations of data in order to determine their differences were made by using one-way analysis of variance (ANOVA) test.

Results and Discussion

Weight Variation, Film Thickness and Tensile Strength of Films Studies for characterization of properties and pharmaceutical quality of films were resulted in data with low standard deviation (S.D.) values which met compendial requirements (Table 3).

Strength of transdermal films were important since they were expected to be enough flexible and to have a mechanical strength on skin for a long time period. Texture analyser results showed that strength of films under the force was in a range of 0.293—0.365 kg/s. It was observed that there was a reverse relationship between tensile strength and molecular weight of semi-synthetic cellulosic polymers such as CMC and HPMC. Increase in PG concentration resulted more flexible films under the force as expected. This can be attributed to plasticizer behaviour of PG in formulations.[11]

FT-IR Analysis FT-IR spectroscopy detects the vibration characteristics of chemical functional groups in a sample. When an infrared light interacts with the matter, chemical bonds will stretch, contract and bend. Therefore, existence of any interaction can be exhibited in order to investigate drug–excipient compatibility.[14] According to the graphs of pure drugs and their transdermal films (MX-HPMC-10 and LX-HPMC-10), drugs and transdermal film excipients were chemically compatible (Figs. 2, 3). Changes in areas of peaks occur simply due to mixing of components independent of any chemical interactions.

Characteristic bands of MX were observed at 1619.34 cm^{-1} (C=0 streching band), 1620—1420 cm^{-1} (C=C streching bands), 1550.51—1064.22 cm^{-1} (C–N streching bands), 1302.38 cm^{-1} (N–C streching band), 1290.98 cm^{-1} and 1162.57—1131.88 cm^{-1} (SO_2 asymmetric and symmetric tension), 1044.20 cm^{-1} (aromatic C–H streching band) and 855.98—650 cm^{-1} (aliphatic C–H vibrations) (Fig. 2a). C–H, N–H and O–H streching bands are also available at 3290.62 cm^{-1}. Main bands of MX were detected with lower intensity caused by PG in the spectrum of MX transdermal patch (Fig. 2b). Broader and sharp peaks indicated secondary and tertiary hydroxyls of PG shealding MX peaks as expected from the matrix structure of the film. However, streching bands and vibrations from MX can be seen in this spectrum. A broader O–H streching band and C–H, N–H and S–H streching bands caused by PG and MX were observed at 3300—3289.68 cm^{-1} and 2970.34—2878.07 cm^{-1}.

Table 3. Weight, Thickness, Tensile Strength and Drug Content of Films

Formulations	W (mg)	t (mm)	S (kg·s)	D (mg)
MX-CMC-7.5	65.33±2.33	0.49±0	0.324±0	2.58±0.14
MX-CMC-10	70.66±1.25	0.55±0.02	0.330±0	2.62±0.08
MX-HPMC-7.5	66.00±0.66	0.50±0	0.293±0	2.60±0.10
MX-HPMC-10	60.02±5.16	0.53±0.01	0.306±0	2.59±0.07
LX-CMC-7.5	64.50±2.55	0.55±0	0.359±0.015	2.60±0.10
LX-CMC-10	65.40±2.20	0.59±0.02	0.365±0.021	2.58±0.07
LX-HPMC-7.5	63.00±0.10	0.60±0.03	0.340±0	2.61±0.07
LX-HPMC-10	62.66±4.32	0.62±0.01	0.351±0	2.59±0.12

W: weight; t: thickness; S: tensile strength; D: drug content; ±S.D.: standard deviation.

Characteristic bands of pure LX were observed at 1645.96 cm^{-1} (C=0 streching band), 1619.50 (aromatic C=C streching band), 1500.93 cm^{-1} (aromatic C=C skeleton streching), 1381.05 cm^{-1} (N–C streching band), 1340.91 cm^{-1} and 1144.75 cm^{-1} (SO_2 asymmetric and symmetric tension), 1325.36—1236.19 cm^{-1} (streching bands of aromatic amine), 1236.19 cm^{-1} (aromatic C–H vibrations) and 764.87 cm^{-1} (C–Cl streching band) (Fig. 3a). C–H, N–H and O–H streching bands are also available at 3101.74—2875.27 cm^{-1}. Main bands of LX were also detected with lower intensity caused by PG in the spectrum of MX transdermal patch (Fig. 3b). A broader O–H streching band at 3341.62 cm^{-1} caused by PG can be seen in the spectrum of LX transdermal patch. C–H, N–H and S–H streching bands of LX with C–H and C–C streching bands of PG were determined at 2971.58—2877.67 cm^{-1}. Broader and sharp peaks indicated secondary and tertiary hydroxyls of PG shealding LX peaks were as detected at 1135.42—1020 cm^{-1}.

C–H streching bands caused by HPMC were detected at 3300—3289.68 cm^{-1} in both of the transdermal film spectrums (Figs. 2b, 3b). R–O–R streching bands and vibrations related to HPMC were not observed in the finger print area due to hydrophilic and lipophilic residues of PG although their presence was known. Data obtained from the spectrums might be indicated decrease in glass transition temperature, T_g, of HPMC.

PG was also thought to affect crystallization behaviours of drugs due to its hydrophilic and lipophilic residues. These findings are supported in part by data obtained from DSC experiments below.

DSC Analysis DSC experiments give information about melting and crystallization behaviour of materials including drugs and excipients. Glass transition processes of polymers, drug–excipient interactions indicating their compatibility and crystallinity degree of drug in films can be determined by DSC.[15] DSC thermograms of MX and LX showed sharp endothermic peaks at 257.7 °C and 227.8 °C corresponding to their melting points, respectively (Fig. 4). Theoretical melting enthalpy of MX and LX were determined as 78.8 J/g and 77.1 J/g. Their melting points decreased to 250.8 °C and 222.8 °C with broader peaks by giving 34.17 J/g and

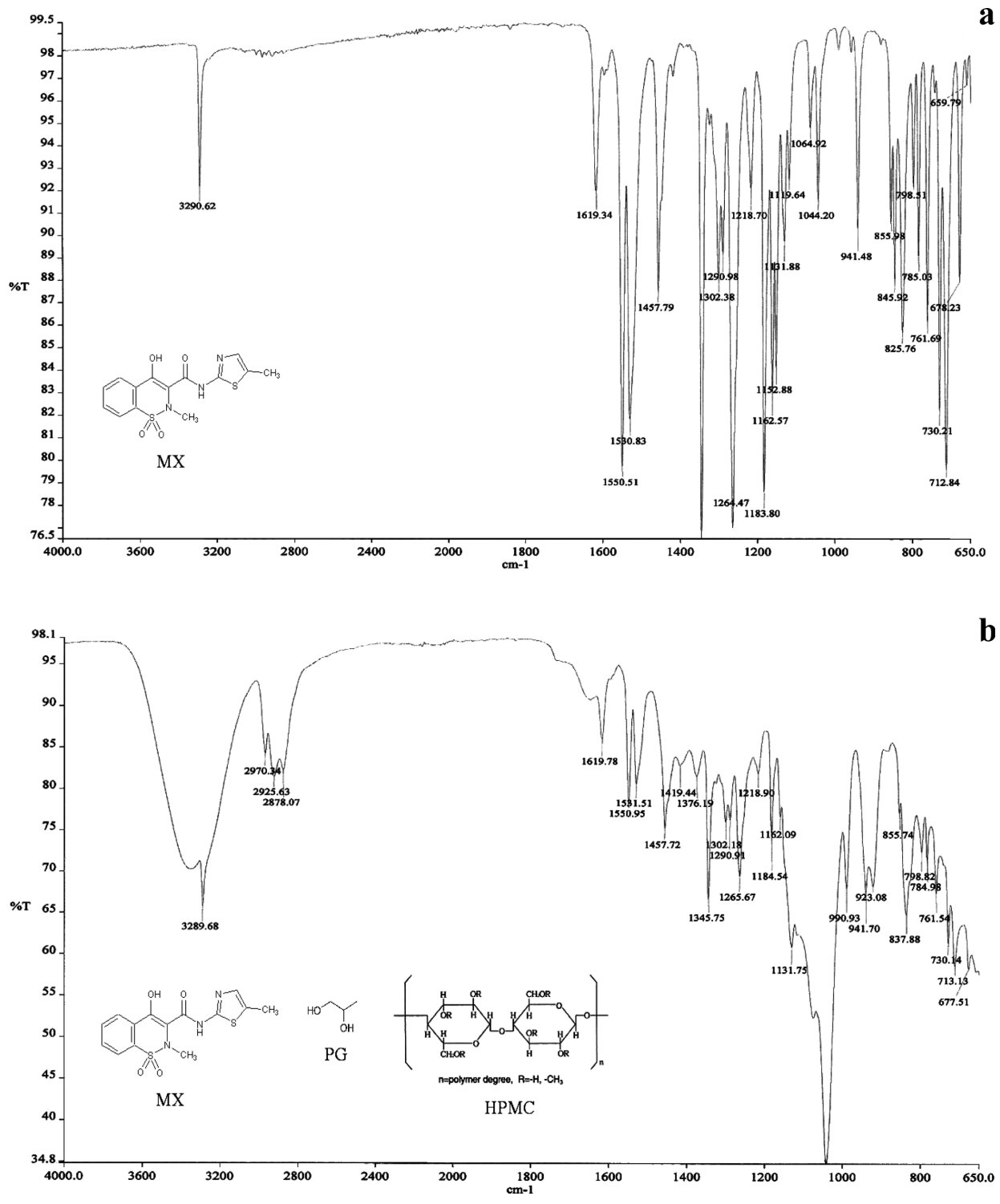

Fig. 2. FT-IR Spectra of Pure MX (a) and Its Transdermal Film (b)

33.71 J/g enthalpies in films. Recrystallization behaviours of drugs in films delayed with addition of PG. Crystalline state of drugs in transdermal films was demonstrated by calculation of crystallinity indice (CI) using following equation[16]:

$$CI(\%) = [me_{sample}/(me_{drug} \times C_{drug})] \times 100 \quad (6)$$

me_{sample}: melting enthalpy of MX and LX in transdermal films; me_{drug}: melting enthalpy of pure MX and LX; C_{drug}: concentration of drugs in transdermal films.

CI of MX and LX was found as 43.36% and 43.72%, respectively. PG was thought to penetrate into the clusters of drug crystals to disorder their arrangements while recrystallization of drugs. All data displayed chemical compatibility between drugs and film ingredients. Any chemical interaction between drugs and film ingredients was not detected. As also expected, addition of PG resulted in decrease in T_g of HPMC which is an important characteristic constant, in particular with respect to applications in the field of controlled

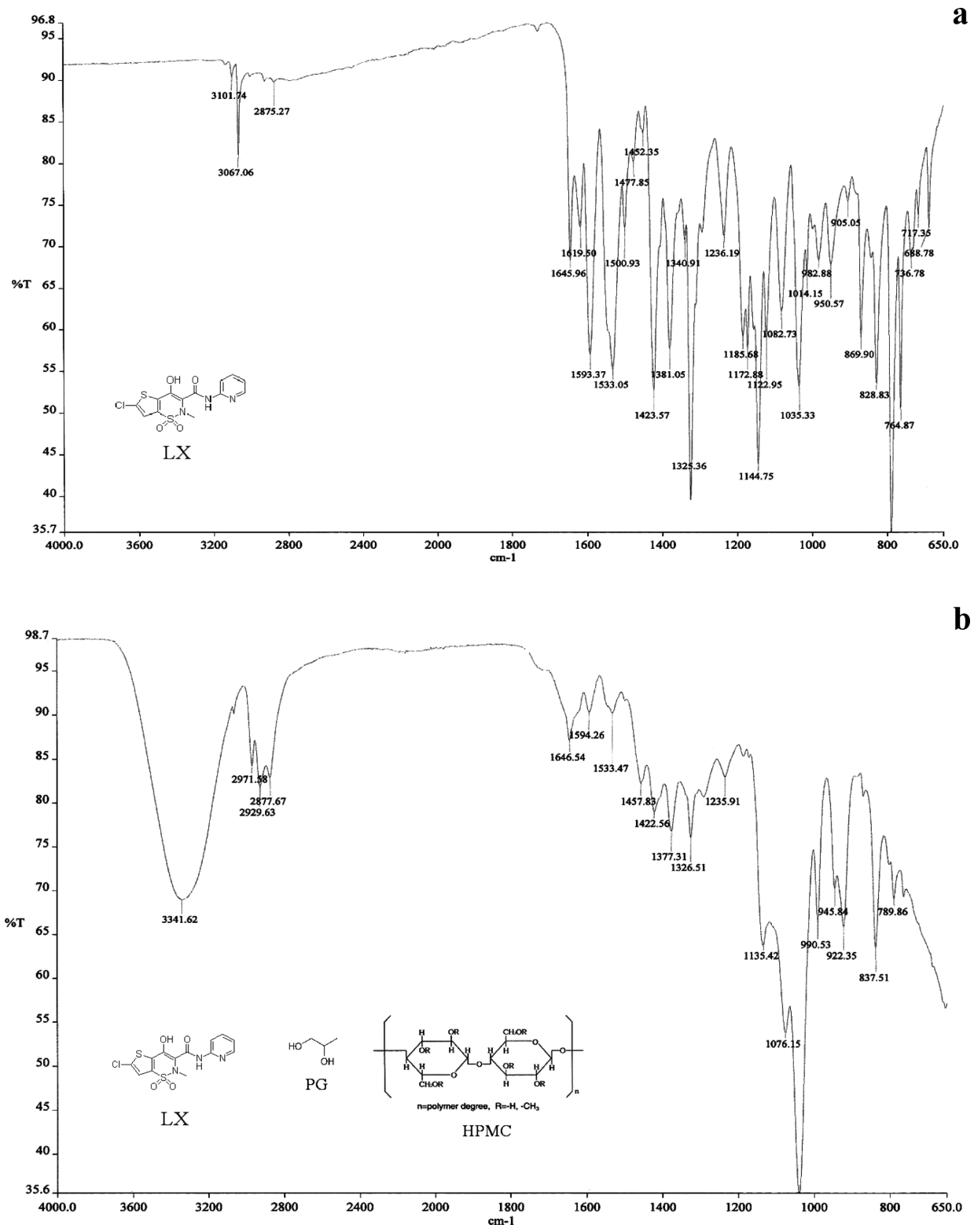

Fig. 3. FT-IR Spectra of Pure LX (a) and Its Transdermal Film (b)

drug delivery. 170—180 °C T_g of HPMC was observed to decrease to 130—140 °C by remaining amorphous.[17,18] Variation in concentration of PG led to small differences on T_g of HPMC.

Drug Content of Films MX and LX films prepared with both of CMC-Na and HPMC displayed homogeneous drug content in matrix structure of the film. Standard deviations from mean drug content were calculated as between 0.07 and 0.14 indicating inconsiderable variations (Table 3).

***In Vitro* Drug Dissolution from Films** *In vitro* dissolution test gives information about drug diffusion through matrix influenced by drug–polymer interaction although it is not correlate with *in vivo* drug release. Moreover, it is one of indicative experiments that is simple and reproduceable for

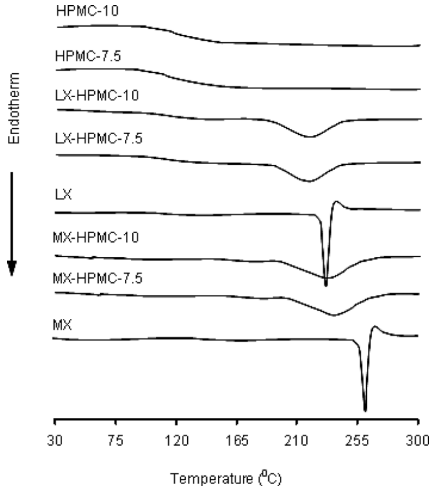

Fig. 4. DSC Curves of Pure MX and LX, Films and Placebo Films

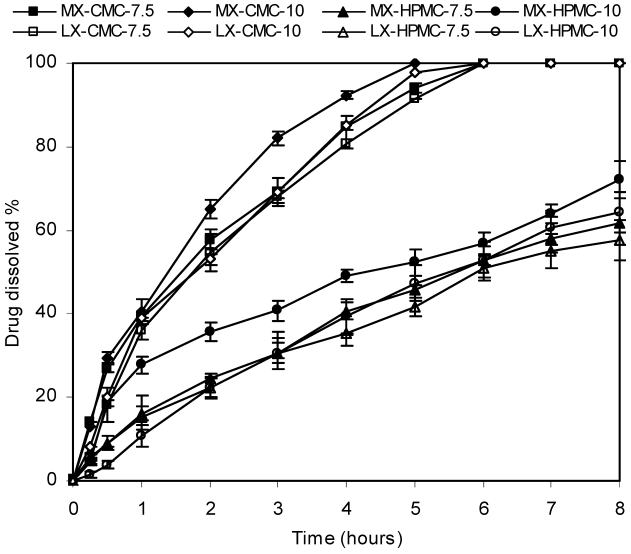

Fig. 5. Dissolution Profiles of MX and LX Films in pH 7.4 PBS

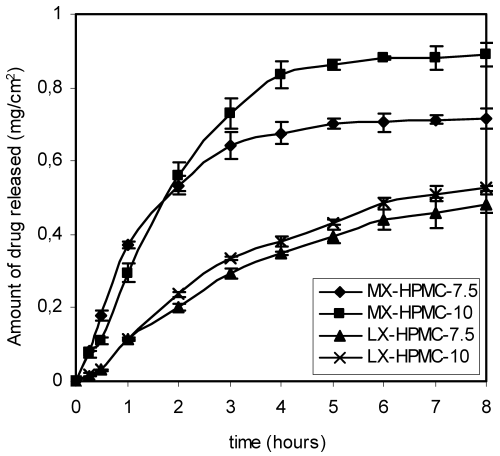

Fig. 6. Release Profiles of MX and LX from Transdermal Patches in pH 7.4 PBS

quality control of finished products.

In vitro dissolution of MX from films was the highest with formulation MX-CMC-10 followed by LX-CMC-10 ($p<0.01$) as can be seen in Fig. 5. Formulations MX-CMC-7.5 and LX-CMC-7.5 displayed insignificantly slower release than formulation LX-CMC-10, but significantly slower than MX-CMC-10 ($p<0.001$). In this study, it was observed that films based on CMC-Na also eroded/disintegrated proportionally by increase in PG concentration. Erosion/disintegration started up to the first hour of the study. CMC-Na formulations containing 7.5% and 10% PG released 100% of drug at the 6th or 5th hours, respectively. This can be attributed to the rapid hydration due to probable formation of hydrophilic micropores in the film structure and subsequent swelling of the polymer. It was important to choose films that maintained their integrity in the medium for 8 h (*i.e.* uneroded/indisintegrated films which allowed release of drug). PG increased mechanical strength of CMC-Na films, but it led to weak matrix structure with the polymer against to aqueous medium. Thus, film disintegration/erosion and rate of drug dissolution were increased with increase in concentration of PG. All films displayed Higuchi model kinetics indicating porous matrix formation. As a result, MX and LX films containing HPMC (MX-HPMC-7.5, MX-HPMC-10, LX-HPMC-7.5 and LX-HPMC-10) were concluded as more advantageous for incorporation into transdermal patches.

***In Vitro* Drug Release from Transdermal Patches** *In vitro* drug release studies were carried out with transdermal patches of HPMC films (MX-HPMC-7.5, MX-HPMC-10, LX-HPMC-7.5 and LX-HPMC-10) since films of CMC-Na displayed insufficient dissolution profiles indicating quality and reproducibility problems as explained in the section, above. Study on *in vitro* drug release from patches through cellulose nitrate membrane showed that MX containing 10% PG (MX-HPMC-10) displayed higher release rate than formulation MX-HPMC-7.5 ($p<0.001$) (Fig. 6). The presence of PG and increase in its concentration in the film accelarated drug diffusion rate probably by formation of hydrophilic micropores in the film structure and by increasing drug solubility.[11,19] Permeability coefficients calculated are presented in Table 4. Drug diffusion through matrix was also thought to be influenced by delayed crystallization behaviour of drugs due to existence of PG in films and PG–polymer interaction indicated in DSC experiment. There was no significant difference between formulations LX-HPMC-7.5 and LX-HPMC-10 as a matter of fact similar thermal behaviours obtained in DSC experiments. Release rates of LX formulations were significantly lower than those of MX formulations. This attitude can be attributed to the difference in *n*-octanol/pH 7.4 buffer partition coefficients of MX and LX as reported as log *P* 0.1 and 1.8, respectively.[20,21]

Cumulative percentage of drug release *versus* square root of time curves shows linearity and it proves that all the formulations follows Higuchi model, suggesting that diffusion may be the mechanism of drug release. The correlation coefficients of Higuchi's plot of formulations are presented in Table 4. Log cumulative percentage of drug release *versus* log time curves shows high linearity and it proves that all the formulations also follow Korsmeyer–Peppas model. The analysis of regression values of Higuchi plot and Korsmeyer–Peppas plot and "*n*" values of Korsmeyer–Peppas model shows a combination of diffusional and dissolutional mechanism indicating the drug release from the formulations

Table 4. Drug Diffusion and Permeability Characteristics of Transdemal Patches

Formulations	Diffusion rate (g/h)×10^3	Permeability coefficient×10^{-3}	Higuchi model r	Korsmeyer–Peppas model r (n)
MX-HPMC-7.5	73.43	1.17	0.9349	0.9515 (0.5905)
MX-HPMC-10	107.06	1.80	0.9591	0.9711 (0.7573)
LX-HPMC-7.5	61.82	1.18	0.9958	0.9831 (0.9929)
LX-HPMC-10	68.04	1.34	0.9942	0.9803 (1.0264)

r: correlation coefficient; n: diffusion exponent of release profile (slope).

was controlled by more than one process. Diffusion exponents of release profiles (slope) from all formulations have values higher than 0.5 indicating release process controlled by non Fickian diffusion.

***In Vivo* Study, Assessment of Anti-inflammatory Effects** Results of *in vivo* study displayed higher anti-inflammatory efficiency with oral suspensions of MX and LX compared to their transdermal patches as expected. Oral suspensions were administered to the rats only with the aim of comparison. One-way ANOVA test emphasized the anti-inflammatory effect of MX from patches was higher than LX from patches as can be seen in Fig. 7. Swelling % was significantly decreased with oral and transdermal application routes compared to blank, Group 1 in general. Comparison of calculated edema inhibition % values are available in Fig. 7. Edema inhibition % of MX patch (Group 3) and LX oral suspension (Group 4) gave similar results up to the end of the fourth hour. However, it should be particularly noted that LX oral suspension displayed higher edema inhibition at the fifth hour indicating oral application of the drug could be expected and estimated to be effective than MX patch.

***Ex Vivo* Skin Penetration Study** Drugs with a log P value below 2.5 are considered to be potential candidates for transdermal delivery.[22,23] The absorption rate increases below this log P value while the absorption rate decreases above this value. MX and LX were reported to have 0.1 and 1.8 log P values (the logarithm of the *n*-octanol/pH 7.4 buffer partition coefficient, P), respectively.[20,21] Therefore, results obtained from MX and LX met expectations on good transdermal penetration (Fig. 8). A significant difference was not found between MX and LX penetration from transdermal patches since there was little correlation between molecular weight and penetration rate in case of drugs within a narrow range of molecular weight (200—500) like NSAIDs as reported in earlier studies. Therefore, major differences in the transdermal absorption was not observed. Smaller molecules such as MX (MW 351.41) and LX (MW 371.82) permeate the skin more rapidly than larger molecules.[23,24]

However, it should be remembered that the use of the organic phase/aqueous phase partition coefficient as a physicochemical parameter in predicting the transdermal absorption of NSAIDs was very useful. However, the log P value can only be used in combination with other indicative parameters such as pK_a (ionization at physiological pH) and solubility constraint.[25] pK_a values for MX and LX were reported as 4.08 and 4.7, respectively.[26,27] An ionizable drug will be present in both charged and uncharged form depending on its pK_a and pH of the environment. The nonionised moiety of a drug is more lipid soluble and may dissolve more rapidly in the lipid material of the skin, thereby facilitating transport by passive diffusion. The ionized moiety, on the other hand, is

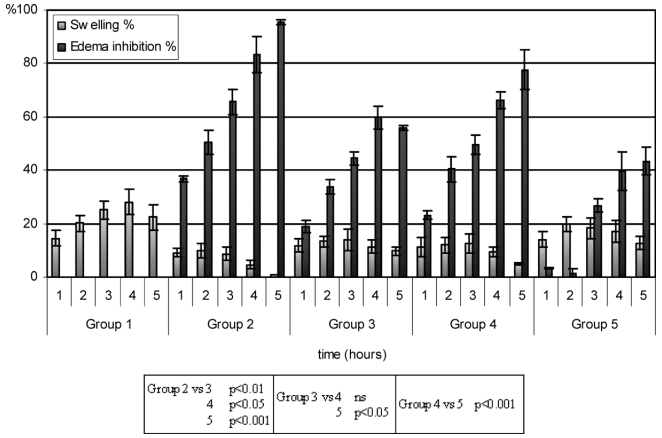

Fig. 7. Swelling % and Edema Inhibition % of MX and LX by Oral and Transdermal Applications to Albino Rats

Comparison of edema inhibition % according to one-way ANOVA test (ns: non-significant).

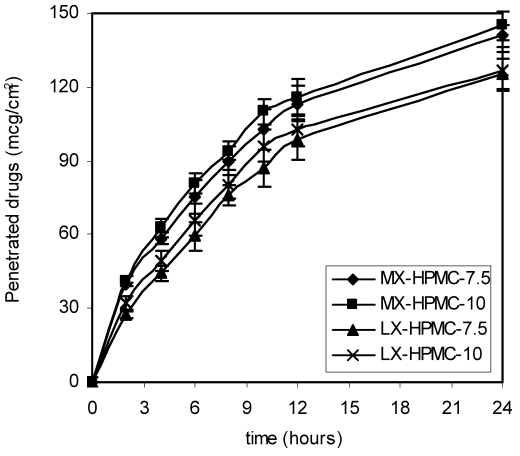

Fig. 8. MX and LX Penetration through Abdominal Skins of Wistar Albino Rats from Transdermal Patches

usually less lipid soluble, limiting transdermal permeation.[13] MX and LX can be assumed to show good penetration to the skin since it can be expected that the nonionised moiety of a drug will penetrate the skin best.

Hadgraft and Wolff reported that the solubility constraint of a drug in the stratum corneum can be defined as the potential a compound may have to form a reservoir in the stratum corneum. When the solubility constraint of a drug is high in stratum corneum, the ultimate systemic availability is expected to be low. Thus, one can predict the rate and extent of absorption into the skin regarding to knowledge of the solubility constraint of the drug.[22] The solubility constraint of MX and LX was calculated as 35.20 and 33.05 indicating

drug retention in the straum corneum and their bioavailibility greater than their counterparts such as ketoprofen (175.38) and ibuprofen (319.15).[22,23)]

Conclusion

It was concluded that the suitable transdermal film formulations for meloxicam (MX) and lornoxicam (LX) were achieved with hydroxypropyl methylcellulose (HPMC) as a polymer and propylene glycol (PG) as a plasticizer. Pharmaceutical quality of transdermal films prepared was proved by physical analysis and FT-IR and DSC experiments. Then, their transdermal patches were prepared.

In vivo studies on rats employed for the assessment of anti-inflammatory effect indicated that MX and LX transdermal patches gave satisfactory results regarding the edema inhibition. MX was found out to be more efficacious compared to LX in case both of oral and transdermal routes. Additionally, LX oral suspension gave the close edema inhibition as MX transdermal patch. All those results were supported by *ex vivo* penetration study in that effects of $\log P$, molecular weight, pK_a and solubility constraint of the relevant drugs were considered.

As a result, transdermal patches of MX and LX can be suggested to be used especially for the immediate treatment of inflammated area since it displays anti-inflammatory effect, soon.

Acknowledgements This study was supported by Research Fund of the Istanbul University. Project number: 2384.

Two parts of this study were presented as posters in 6th World Meeting on Pharmaceutics, Biopharmaceutics and Pharmaceutical Technology (Barcelona, Spain, 7—10 April 2008) and 7th World Meeting on Pharmaceutics, Biopharmaceutics and Pharmaceutical Technology (Valetta, Malta, 8—11 March 2010).

References

1) Turner P., Johnston A., *Postgrad. Med. J.*, **66**, 28—29 (1990).
2) Balfour J. A., Fitton A., Barradell L. B., *Drugs*, **51**, 639—657 (1996).
3) Meineke I., Turck D., *Br. J. Clin. Pharmacol.*, **55**, 32—38 (2003).
4) Olkkola K. T., Brunetto A. V., Mattila M. J., *Clin. Pharmacokinet.*, **26**, 107—120 (1994).
5) Aronson J. K., "Meyler's Side Effects of Drugs: The International Encyclopedia of Adverse Drug Reactions and Interactions," Elsevier, Amsterdam, 2006, pp. 2167—2168.
6) Aronson J. K., "Meyler's Side Effects of Drugs: The International Encyclopedia of Adverse Drug Reactions and Interactions," Elsevier, Amsterdam, 2006, pp. 2248—2249.
7) Yakhno N., Guekht A., Skoromets A., Spirin N., Strachunskaya E., Ternavsky A., Olsen K. J., Moller P. L., *Clin. Drug Investig.*, **26**, 267—277 (2006).
8) Baker R. W., Heller J., "Materials Selection for Transdermal Delivery Systems," STS Publishing, U.K., 1992.
9) Williams A. C., "Transdermal and Topical Drug Delivery—From Theory to Clinical Practice," Pharmaceutical Press, London, 2003.
10) Kılıç P., "Meloksikam ve Lornoksikam Içeren Topikal Formülasyonlar Üzerine Çalışmalar," M. Sc., Thesis. Istanbul University, Istanbul, 2008.
11) Rao P. R., Diwan P. V., *Pharm. Acta Helv.*, **72**, 47—51 (1997).
12) Korsmeyer R. W., Gurny R., Doelker E., Buri P., Peppas N. A., *Int. J. Pharm.*, **15**, 25—35 (1983).
13) Ritschel W. A., "Drug Delivery Devices, Fundamentals and Applications," ed. by Tyle P., Marcel Dekker, New York, 1988.
14) Stott O. W., Williams A. C., Barry B. W., *J. Controlled Release*, **50**, 297—308 (1998).
15) Ford J. L., Timmins P., "Pharmaceutical Thermal Analysis," Ellis Horwood, Chichester, 1989.
16) Teeranachaideekul V., Müller R. H., Junyaprasert V. B., *Int. J. Pharm.*, **340**, 198—206 (2007).
17) Kibbe A., "Handbook of Pharmaceutical Excipients," American Pharmaceutical Assocciation and Pharmaceutical Press, New York, 2000.
18) Siepmann J., Peppas N. A., *Adv. Drug Deliv. Rev.*, **48**, 139—157 (2001).
19) Guyot M., Fawaz F., *Int. J. Pharm.*, **204**, 171—182 (2000).
20) Galani A., Demertzis M. A., Kubicki M., Kovala-Demertzi D., *Eur. J. Inorg. Chem.*, **2003**, 1761—1767 (2003).
21) Oliveira E. F. S., Azevedo R. C. P., Bonfilio R., Oliveira D. B., Ribeiro G. P., Araujo M. B., *Brazil. J. Pharm. Sci.*, **45**, 67—73 (2009).
22) Hadgraft J., Wolff M., "Dermal and Transdermal Drug Delivery," ed. by Gurny R., Teubner A., Wissenschaftliche Verlagsgesellschaft, Stuttgart, 1993, pp. 161—172.
23) Beetge E., du Plessis J., Müller D.G., Goosen C., van Rensburg F. J., *Int. J. Pharm.*, **193**, 261—264 (2000).
24) "The Merck Index," 14th ed., Merck and Co., Inc., U.S.A., 2006.
25) Goosen C., du Plessis J., Müller D. G., van Rensburg L. F. J., *Int. J. Pharm.*, **163**, 203—209 (1998).
26) Prasad Byrav D. S., Medhi B., Prakash A., Patyar S., Wadhwa S., *Drug Rev.*, **20**, 27—31 (2009).
27) Snor W., Liedl E., Weiss-Greiler P., Viernstein H., Wolschann P., *Int. J. Pharm.*, **381**, 146—152 (2009).